A Novel Approach for Screening the Proteome for Changes in Protein Conformation†

Anson Pierce,‡ Eric deWaal,§ Holly Van Remmen,‡,||,⊥ Arlan Richardson,‡,||,⊥ and Asish Chaudhuri*,§,||,⊥

Departments of Cellular and Structural Biology and Biochemistry and Barshop Institute for Longevity and Aging Studies, University of Texas Health Science Center at San Antonio, San Antonio, Texas 78229, and the Geriatric Research Education and Clinical Center, South Texas Veterans Health Care System, San Antonio, Texas 78284

Received October 6, 2005; Revised Manuscript Received January 12, 2006

ABSTRACT: Changes in surface hydrophobicity are generally considered as a sensitive indicator for monitoring the structural alterations of proteins that are often associated with changes in function. Currently, no technique has been developed to screen a complex mixture of proteins for changes in the conformation of specific proteins. In this study, we adapted a UV photolabeling approach, using an apolar fluorescent probe, 4,4′-dianilino-1,1′-binaphthyl-5,5′-disulfonic acid (BisANS), to monitor changes in surface hydrophobic domains in either purified rhodanese or skeletal muscle cytosolic proteins by urea-induced unfolding or in response to *in vitro* metal-catalyzed oxidation. Using two-dimensional polyacrylamide gel electrophoresis (2D PAGE), we identified two specific proteins in skeletal muscle cytosol that exhibited a marked loss of incorporation of BisANS after exposure to *in vitro* oxidative stress: creatine kinase (CK) and glyceraldehyde-3-phosphate dehydrogenase (GAPDH). We found that the activities of both enzymes were also reduced significantly in response to oxidative stress. We then determined if this method could detect changes in surface hydrophobicity in specific proteins arising from oxidative stress generated *in vivo* by muscle denervation. A loss in surface hydrophobic domains in CK and GAPDH was again observed as measured by the BisANS photoincorporation approach. In addition, the CK and GAPDH activity in denervated muscle was markedly reduced. These data demonstrate for the first time that this assay can screen a complex mixture of proteins for alterations in surface hydrophobic domains of individual proteins.

Maintenance of the functional structure of the protein is one of the key determinants for normal homeostasis in cells and tissues. Numerous tools are available to measure the conformational state of proteins including circular dichroism (*1*), nuclear magnetic resonance (*2*), fluorescence polarization (*3*), and light scattering (*4*). Conformational changes in proteins are often associated with the exposure of hydrophobic amino acids on the surface (*5*), which may lead to changes in protein function, or the initiation of aggregation, whereby hydrophobic domains become sequestered within oligomeric structures (*6*). Changes in surface hydrophobicity of proteins have been exploited as a way to study and characterize the conformational state of individual proteins to determine how changes in the structure affect function. A variety of methods have been used to monitor changes in surface hydrophobicity, e.g., hydrophobic interaction chromatography (*7*), surface plasmon resonance (*8*), and incorporation of hydrophobic fluorescent dyes such as anilinoline sulfonate (ANS)[1] compounds that bind to hydrophobic domains (*9*).

The use of fluorescent dyes to monitor surface hydrophobicity is advantageous because of their ease of use. ANS compounds have been in use since 1952 (*10*) to study the changes on the surface hydrophobicity of purified proteins in response to various conditions such as hydrostatic pressure (*11*, *12*), heat (*13*), pH (*14*), and denaturation (*15*). ANS and its derivative, 4,4′-dianilino-1,1′-binaphthyl-5,5′-disulfonic acid (BisANS), bind preferentially and reversibly to hydrophobic pockets on the surface of proteins, and this interaction gives fluorescence maxima at 490 nm when excited at 385 nm (*16*−*18*). Using the purified protein GroEL, Seale et al. (*19*) showed that BisANS could be covalently bound to the site of interaction by irradiating the sample with longwave

† This work was supported by a VA-VISN grant (to A.C.) and a REAP grant from the Department of Veteran Affairs (to H.VR., A.R., and A.C.), P01 AG19316 (to A.R.) and R01-AG23843 (to A.R.) grants from the National Institute of Aging, and a grant from the Ellison Medical Foundation (to A.R.).

* To whom correspondence should be addressed: Department of Biochemistry, University of Texas Health Science Center, 7703 Floyd Curl Drive, San Antonio, TX 78229. E-mail: chaudhuria@uthscsa.edu. Telephone: 210-617-5300 ×5556. Fax: 210-567-4414.

‡ Department of Cellular and Structural Biology, University of Texas Health Science Center at San Antonio.

§ Department of Biochemistry, University of Texas Health Science Center at San Antonio.

|| Barshop Institute for Longevity and Aging Studies, University of Texas Health Science Center at San Antonio.

⊥ South Texas Veterans Health Care System.

[1] Abbreviations: BisANS, 4,4′-dianilino-1,1′-binaphthyl-5,5′-disulfonic acid; CK, creatine kinase; GAPDH, glyceraldehyde-3-phosphate dehydrogenase; MALDI−TOF/MS, matrix-assisted laser desorption ionization time-of-flight mass spectrometry; ANS, anilinoline sulfonate; UV, ultraviolet; PAGE, polyacrylamide gel electrophoresis; TCA, trichloroacetic acid; Hepes, 4-(2-hydroxyethyl)piperazine-1-ethanesulfonic acid; MCO, metal-catalyzed oxidation; IPG, immobilized pH gradient, CHAPS, 3-[(3-cholamidopropyl)dimethylammonio]-1-propanesulfonate.

10.1021/bi052031i CCC: $33.50
Published on Web 02/07/2006

ultraviolet (UV) light. Two studies have examined the site of incorporation of BisANS into proteins and found that at most 2 BisANS molecules covalently bind to peptides within the protein after photolabeling with BisANS (*19*, *20*).

We have taken advantage of the ability of BisANS to recognize hydrophobic domain(s) within proteins and to become covalently bound to these sites after UV irradiation to develop a proteomic-based assay that allows one to screen the proteome for changes in the conformation of individual proteins using unoxidized and *in vitro* oxidized skeletal muscle cytosolic proteins as a model system. In addition, we show that through BisANS incorporation we can detect changes in surface hydrophobicity in specific proteins in an *in vivo* model of oxidative stress. We consistently observed in both the *in vitro* and *in vivo* models of oxidative stress changes in surface hydrophobicity and activity in two major skeletal muscle proteins, creatine kinase (CK) and glyceraldehyde-3-phosphate dehydrogenase (GAPDH).

EXPERIMENTAL PROCEDURES

Materials. BisANS and Sypro Ruby protein gel stain were purchased from Molecular Probes (Junction City, OR). Tris base, $MgCl_2$, urea, trichloroacetic acid (TCA), and ethyl acetate were purchased from EMD Chemicals (Gibbstown, NJ). EDTA was purchased from Gibco BRL, and [4-(2-hydroxyethyl)piperazine-1-ethanesulfonic acid] (Hepes) and iodoacetamide were purchased from Sigma (Dallas, TX). Coomassie Blue stain was purchased from BioRad, and protease cocktail inhibitor was purchased from Calbiochem (San Diego, CA). The BCA assay kit was purchased from Pierce (Rockland, IL). Immobilized pH gradient (IPG) buffer and 3-[(3-cholamidopropyl)dimethylammonio]-1-propanesulfonate (CHAPS) were purchased from Amersham (Piscataway, NJ), and trypsin (modified) was from Promega (Madison, WI). The Montage in-gel digest kit was purchased from Millipore (Billerica, MA).

Methods: Animals and Animal Procedures. Male C57Bl/6J mice (4−6 months) were used as the source of gastrocnemius and tibialis anterior skeletal muscle protein for *in vitro* studies. For denervation studies, mice were anesthetized using isoflurane. The left hind limb was shaved and disinfected with iodine, and the sciatic nerve was isolated and cut through a small incision. A 0.2 cm piece was removed, and the ends of the nerve were folded back and sutured with 7.0 silk to prevent re-innervation. The incision was closed with wound clips, and the mouse was allowed to recover. After 21 days, mice were sacrificed and the gastrocnemius muscle from the right leg (control) and denervated (left leg) were removed and frozen in liquid nitrogen. All procedures for handling animals in this study were reviewed and approved by the IACUC (Institutional Animal Care and Use Committee) of The University of Texas Health Science Center at San Antonio and the IACUC of Audie L. Murphy Memorial Veterans Hospital.

In Vitro Oxidation of Proteins. Oxidation of rhodanese was carried out essentially as described by Chao et al. (*21*). Gastrocnemius and tibialis regions of the skeletal muscle were homogenized in 50 mM Tris-HCl at pH 7.4 containing 10 mM $MgSO_4$ and protease inhibitors and centrifuged at 100000*g* for 1 h at 4 °C. The cytosolic proteins were diluted to 1 mg/mL in various concentrations of oxidizing solution ranging from 0 to 40 μM $FeSO_4$ and 0 to 10 mM ascorbate, maintaining a constant 1:250 ratio of $FeSO_4$/ascorbate in 100 mM KCl, 100 mM $MgSO_4$, and 50 mM Hepes at pH 7.2. Oxidation was carried out for 1 h at 37 °C in the dark. Protein concentrations were determined by the Bradford method (*22*).

UV-Induced Photoincorporation of BisANS to Proteins. Photoincorporation of BisANS was carried out as described by Seale et al. (*19*). The clear cytosolic protein extracts were diluted to 1 mg/mL in labeling buffer containing 50 mM Tris-HCl, 10 mM $MgSO_4$ at pH 7.4, and protease inhibitors. Then, 100 μM BisANS was added, and samples were immediately vortexed. Next, 200 μL of sample was added to a clear 96-well plate and incubated on ice (to minimize local heating) for 1 h under direct exposure of a 115 V 0.16 Amp handheld longwave UV lamp (365 nm; Ultraviolet Products, Inc., model UVL-21). Using this setup, there was a distance of 7 mm between the light source and the top of the sample, which had a depth of 6.25 mm when 200 μL was loaded. After the photoincorporation of BisANS, proteins were then dissolved in Laemmli buffer (*23*) and subjected to SDS−polyacrylamide gel electrophoresis (PAGE). During SDS−PAGE, unbound BisANS in the sample migrates with the dye front and is consequently removed. After electrophoresis, gels were removed and illuminated with 365 nm UV light and BisANS fluorescence was captured with an AlphaImage 3400 for quantification.

Two-Dimensional Gel Electrophoresis. For 2D gel electrophoresis, BisANS-labeled proteins (control and experimental samples) were treated with an equal volume of 20% TCA for 10 min on ice and centrifuged at 16000*g* for 15 min at 25 °C. The pellets were then washed with a mixture of ethanol/ethyl acetate (1:1, v/v) at least 3 times to remove the unbound BisANS. After removal of the BisANS, the pellets were then dissolved in lysis buffer containing 8 M urea, 4% CHAPS, and 2% IPG buffer at pH 3.0−10. The protein concentration was measured by the BCA assay. Approximately 100 μg of protein was loaded in 250 μL of rehydration buffer containing 8 M urea, 2% CHAPS, 0.5% IPG buffer, 1% bromophenol blue, and 2.4 mg/mL DTT. The first dimension of electrophoresis was run on 13 cm strips (pH 3−10) using the IPGphor Isoelectric Focusing System overnight. After the first dimension, strips were washed in equilibration buffer (50 mM Tris buffer at pH 8.8, 6 M urea, 30% glycerol, 2% SDS, and 0.002% bromophenol blue). Strips were then washed twice for 15 min, first with DTT (100 mg/mL) and second with iodoacetamide (250 mg/mL). The second dimension was run on 12% SDS−PAGE gels. After electrophoresis, gels were removed and illuminated with long-wave UV light and the image was captured with an AlphaImage 3400. Gels were then fixed with 10% methanol and 7% acetic acid for 10 min followed by staining overnight with Sypro Ruby. The stained gels were washed in 10% methanol and 7% acetic acid for 30 min to remove residual dye and placed in water. The Typhoon 9400 variable mode imager with excitation at 532 nm and an emission filter of 610BP30 was used to scan the gels. Scanned gels for BisANS fluorescence (obtained from AlphaImage 3400) and Sypro Ruby fluorescence (obtained from Typhoon 9400 variable mode imager) were quantitated separately from 16-bit gray-scale images using Imagequant version 5.0 (Molecular Dynamics, Amersham,

Piscataway, NJ). The background was corrected for each spot using the object average function. The background-corrected pixel intensities of BisANS and Sypro fluorescence were divided by their respective size-matched elliptical areas. To normalize BisANS fluorescence for protein expressional changes, the pixel intensity/area for BisANS fluorescence was divided by the pixel intensity/area of Sypro Ruby fluorescence.

Matrix-Assisted Laser Desorption Ionization Time-of-Flight Mass Spectrometry (MALDI−TOF/MS). Spots of interest were excised from the 2D gels and digested *in situ* with modified trypsin (15 μL of 55 μg/mL). The peptides were concentrated and purified further using a Montage in-gel digest kit. The resulting digests were analyzed by MALDI−TOF/MS using an Applied Biosystems Voyager DE-STR on a Thermo Finnigan LCQ. MALDI−TOF mass spectra were generated by the summation of 100 laser shots. Unmodified peptides produced from tryptic digestion were used as the criteria to identify the protein. Peptides were matched using Mascot against the NCBInr database, with carbamidomethyl and methionine oxidation as variable modifications. Peptide tolerance was set at 75 ppm, and scores above 64 were considered significant.

Enzyme Activities. To measure the enzyme activities of CK and GAPDH, the solutions containing oxidized or unoxidized proteins were directly applied to a Centricon 10 microconcentrator (Amicon, Inc., MA) to remove the excess $FeSO_4$ and ascorbate from oxidized samples and diluted in equivalent volumes of 50 mM Tris-HCl and 10 mM $MgSO_4$ at pH 7.4 before proceeding to measure the enzyme activity. CK was measured spectrophotometrically in an enzyme-coupled system as described by Tanzer and Gilvarg (*24*). The assay was carried out at room temperature by adding 700 μL of a solution containing 8.5 mM ATP, 1.22 mM NADH, 2.0 mM phosphoenol pyruvate, 15 units/mL lactate dehydrogenase, 7 units/mL pyruvate kinase, 28 mM $MgSO_4$, and 26 mM reduced glutathione at pH 7.4, combined with 2.2 mL of buffered creatine containing 0.4 M glycine, 53.2 mM creatine, and 62 mM potassium carbonate at pH 8.9. Activity was measured at 340 nm by the rate of NADH oxidation for 13 min every 30 s by adding 0.1 mL of tissue extract containing 0.05 mg of protein/mL in 5 mM glycine at pH 9.0. Enzyme units were calculated by the extinction coefficient of NADH, where 1 unit is equal to the amount of enzyme required to convert 1 μmol of creatine to creatine phosphate/min at 25 °C and pH 8.9. GAPDH was measured spectrophotometrically as described by Rafter et al. (*25*) and Harting Velick (*26*). Muscle cytosolic protein extracts were diluted in 15 mM sodium pyrophosphate/30 mM sodium arsenate buffer at pH 8.5 to 0.05 mg of protein/mL, and 0.1 mL of tissue extract was added to a cuvette containing 2.6 mL of pyrophosphate/arsenate buffer containing 0.015 M sodium pyrophosphate, 0.03 M sodium arsenate at pH 8.5, 0.1 mL of 7.5 mM NAD, and 0.1 mL of 0.1 M DTT. Absorbance was monitored at 340 nm, and enzyme units were calculated by the extinction coefficient of NADH, where 1 unit is equal to the amount of enzyme required to convert 1 μmol of glyceraldehyde-3-phosphate to 1,3-bisphosphoglycerate/min at 25 °C and pH 8.5.

Isolation of Mitochondria and Measurement of H_2O_2 Production. Skeletal muscle mitochondria were purified as described by Chappell and Perry (*27*) and were used immediately after isolation. Mitochondrial H_2O_2 release was measured using the fluorogenic probe Amplex Red (Molecular Probes, OR) in conjunction with horseradish peroxidase as described by Muller et al. (*28*). H_2O_2 release was measured in isolated muscle mitochondria incubated in the absence of exogenous substrate (state 1) or in the presence of 5 mM potassium glutamate plus potassium malate as respiratory substrates.

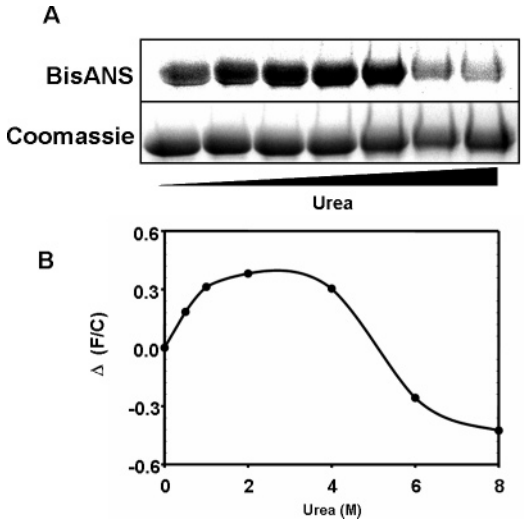

FIGURE 1: Effect of urea on rhodanese surface hydrophobicity. Purified rhodanese (1 mg/mL) was incubated with increasing concentrations of urea (0, 0.5, 1, 2, 4, 6, and 8 M) for 1 h at 37 °C followed by labeling with 100 μM BisANS and SDS−PAGE. The fluorescence from BisANS and image from Coomassie Blue were captured as described in the Experimental Procedures. (A) Image of the region of the gel containing rhodanese, showing the fluorescence from BisANS and the Coomassie Blue stain. (B) BisANS fluorescence (*F*) was quantitated by densitometry and normalized by Coomassie staining (*C*). Data are expressed as the change in fluorescence intensity ($\Delta F/C$).

Statistical Analysis. The data were analyzed using Student's *t* test with the Winstat add-in (Microsoft Excel) or using one-way ANOVA with Dunett's post hoc test for multiple comparisons. Statistical significance was set at the $p \leq 0.05$ level.

RESULTS

Detection of Changes in Surface Hydrophobicity of Rhodanese by BisANS Photoincorporation after Denaturation or Oxidation. The purified mitochondrial protein rhodanese was used as a model protein to determine if the changes in surface hydrophobicity induced by various treatments can be detected by photoincorporation of BisANS. Rhodanese was treated with increasing concentrations of urea (0−8 M) followed by photolabeling of rhodanese with BisANS and subjected to SDS−gel electrophoresis (Figure 1). The fluorescence intensity of BisANS-labeled rhodanese exhibited a bell-shaped pattern in response to an increased concentration of urea, with a maximum intensity ($\Delta F/C$) observed at 2 M urea, which is indicative of the formation of stable intermediate complexes with increased surface hydrophobicity. At urea concentrations above 4 M, a dramatic decrease in BisANS incorporation is observed, which is likely due to the unfolding of the rhodanese protein. Thus, changes in BisANS incorporation correlate with the structural alterations of rhodanese by urea-induced unfolding.

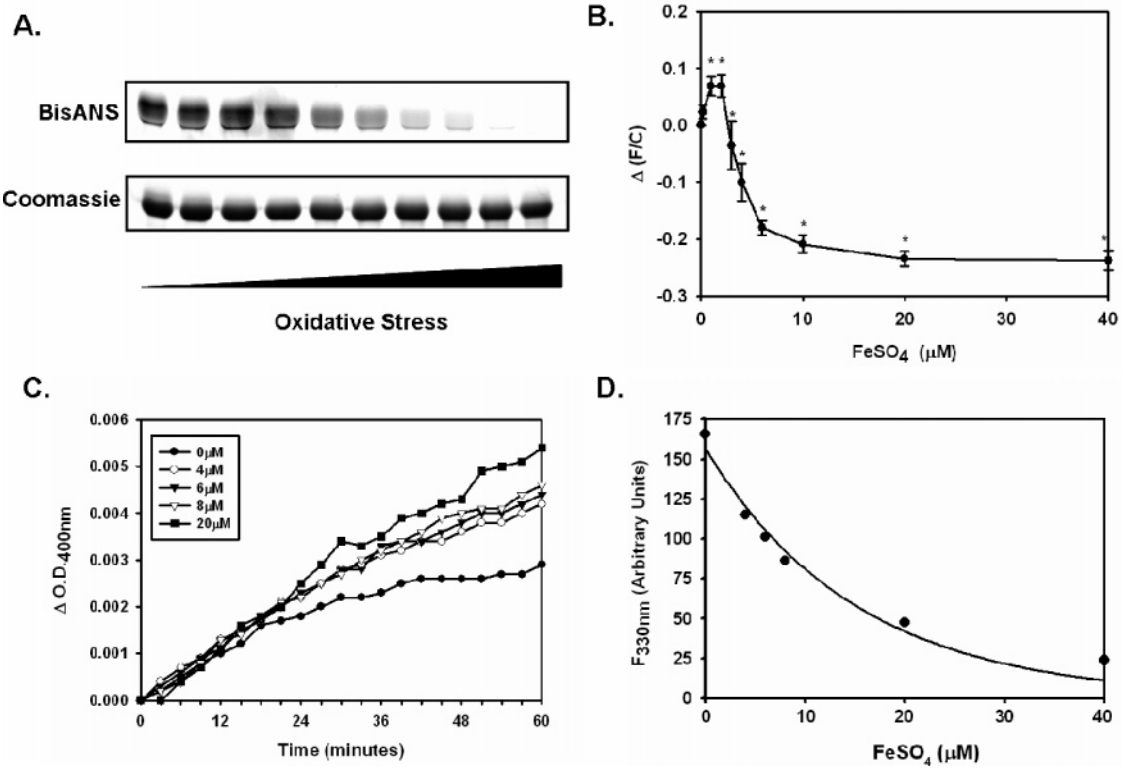

FIGURE 2: Effect of MCO on rhodanese surface hydrophobicity and aggregation. Purified rhodanese (1 mg/mL) was incubated with increasing concentrations of iron (0, 0.2, 1.0, 2.0, 3.0, 4.0, 6.0, 8.0, 20, and 40 μM) and ascorbate (0, 0.05, 0.25, 0.5, 0.75, 1, 1.5, 2.5, 5, and 10 mM) for 1 h at 37 °C followed by labeling with 100 μM BisANS and then SDS−PAGE. The fluorescence from BisANS and staining from Coomassie Blue on the gels was determined as described in the Experimental Procedures. (A) Image of the BisANS fluorescence and Coomassie Blue stained region of the gel containing rhodanese. (B) BisANS fluorescence (*F*) and Coomassie Blue stain (*C*) in A were quantified by densitometry as described in the Experimental Procedures, and the data are expressed as the average ($n = 3$) change in fluorescence intensity ($\Delta F/C$) of the untreated and treated samples ± standard deviation. (*) $p \leq 0.05$ versus the control. (C) Light scattering of rhodanese was measured by ΔOD_{400} as described in the Experimental Procedures over time at the various concentrations of oxidative stress shown. (D) Tryptophan fluorescence quenching was measured at 330 nm as described in the Experimental Procedures at various concentrations of iron/ascorbate.

Next, rhodanese was used as a model to examine the impact of oxidation on BisANS incorporation. This was achieved using a metal-catalyzed oxidation (MCO) system involving iron and ascorbate as a generator of hydroxyl radicals. Parts A and B of Figure 2 show that BisANS incorporation into rhodanese was increased significantly at low levels of oxidative stress (3 μM/0.75 mM iron/ascorbate). Increasing concentrations of iron/ascorbate resulted in a progressive loss of BisANS fluorescence. The chance of photo or chemical bleaching of BisANS fluorescence by urea and MCO alone was ruled out by the fact that neither the quantum yield nor the emission maxima of BisANS were affected by the treatment with urea and MCO (data not shown). In addition, protein oxidation may have induced peptide bond cleavage in samples oxidized with 40 μM/10 mM iron/ascorbate (*29*), as evidenced by the slight reduction in Coomassie staining (Figure 2A). Because one of the likely explanations for reduction in incorporation of BisANS to the surface hydrophobic regions of rhodanese with increasing oxidative stress is protein aggregation, light scattering and tryptophan fluorescence quenching experiments were performed with rhodanese in the presence of different concentrations of iron/ascorbate (parts C and D of Figure 2). Rhodanese showed a MCO concentration-dependent increase in absorbance at 400 nm as well as the loss of tryptophan fluorescence at 330 nm when excited at 296 nm. These data indicate that free radicals generated by the MCO reaction trigger the formation of higher order structures using domains exposed during the oxidative stress state, leading to a reduction in BisANS photoincorporation to rhodanese.

Monitoring Changes in Protein Conformation in Tissue Extracts by Photoincorporation of BisANS. We next determined whether BisANS could be used as a screening probe for monitoring conformational alterations in a complex mixture of proteins. Cytosolic extracts were treated with various concentrations of iron/ascorbate followed by photolabeling of proteins with BisANS. The global level of incorporation of BisANS to the cytosolic proteins was determined by SDS−gel electrophoresis as shown in Figure 3A. A bell-shaped pattern of BisANS fluorescence was observed for the total incorporation of BisANS to the skeletal muscle cytosolic proteins (Figure 3C). At higher levels of oxidative stress (above 2 μM/0.25 mM iron/ascorbate), a dramatic decrease in global BisANS incorporation into cytosolic proteins was observed.

We next asked if we could detect changes in the incorporation of BisANS to individual proteins in the cytosolic extracts from skeletal muscle. In these experiments, the extracts were untreated or treated with low (0.2 μM $FeSO_4$/0.05 mM ascorbate) and high (40 μM $FeSO_4$/10 mM ascorbate) levels of oxidative stress and the proteins in the extract were resolved by 2D gel electrophoresis. The data in Figure 4 show that we could monitor changes in the incorporation of BisANS into individual proteins in response

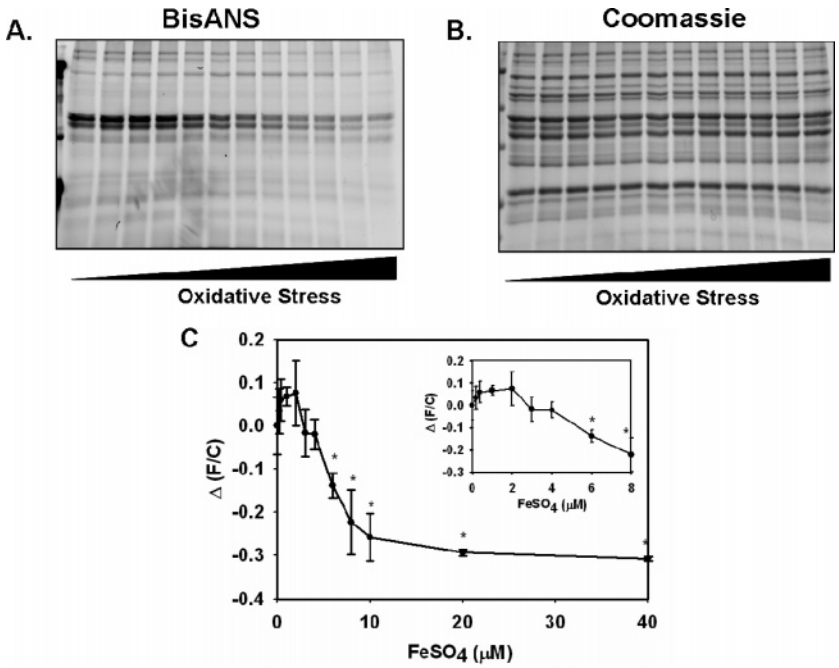

FIGURE 3: Detection of changes in surface hydrophobicity in cytosolic proteins from skeletal muscle after oxidative stress. Extracts of cytosolic proteins (1 mg/mL) from mouse skeletal muscle were exposed to increasing concentrations of iron (0, 0.2, 0.4, 1.0, 2.0, 3.0, 4.0, 6.0, 8.0, 10, 20, and 40 μM) and ascorbate (0, 0.05, 0.1, 0.25, 0.5, 0.75, 1, 1.5, 2, 2.5, 5, and 10 mM) for 1 h at 37 °C followed by labeling with 100 μM BisANS and then SDS−PAGE. The fluorescence from BisANS and staining from Coomassie Blue in the gels was determined as described in the Experimental Procedures. (A) Image of the gel showing the fluorescence from BisANS. (B) Image of the gel showing Coomassie Blue stained protein labeled with BisANS. (C) BisANS fluorescence (*F*) and Coomassie Blue staining (*C*) in A and B were quantified by densitometry as described in the Experimental Procedures, and the data are expressed as the average ($n = 3$) change in fluorescence intensity ($\Delta F/C$) of the untreated and treated sample ± standard deviation. (*) $p \leq 0.05$ versus the control.

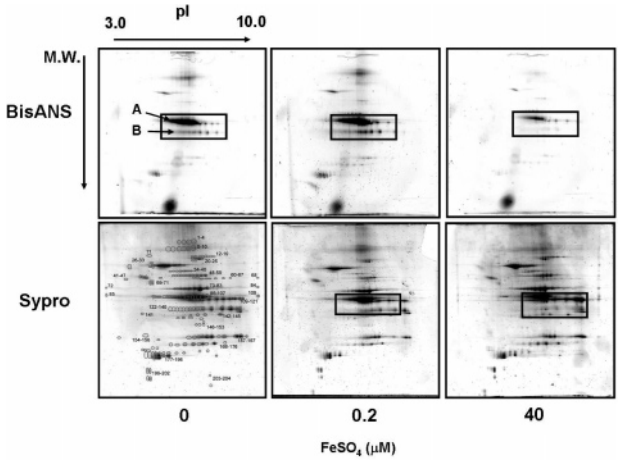

FIGURE 4: Screen of the skeletal muscle cytosolic proteome for changes in surface hydrophobicity after oxidative stress. Cytosolic extracts (1 mg/mL) from mouse skeletal muscle were exposed to iron (0, 0.2, and 40 μM) and ascorbate (0, 0.05, and 10 mM) for 1 h at 37 °C followed by labeling with 100 μM BisANS and then 2D gel electrophoresis. The fluorescence from BisANS and Sypro Ruby on the gels was determined as described in the Experimental Procedures. The 204 spots that were analyzed are circled in the bottom left gel, and regions of interest are boxed, showing two apparent pI variants indicated by A and B.

to oxidative stress. To quantify these changes, the fluorescence because of BisANS in each spot was divided by the Sypro Ruby fluorescence, a measure of the level of protein in the spot. We measured the changes in BisANS incorporation in individual proteins by calculating the ratio of BisANS/Sypro Ruby fluorescence in 204 spots before and after a low and high level of oxidative stress, and these data are given in Figure 5. We focused on two pI variants (indicated as A and B in Figures 4 and 5) that are highly expressed in skeletal muscle and were found to show pronounced changes in surface hydrophobicity with oxidative stress. Six spots were picked from the parent proteins in the two regions of interest (indicated by arrows in Figure 5) and shown in Figure 6A. Tryptic digests from these spots were analyzed by MALDI−TOF/MS, and representative mass spectra of these spots are shown in Figure 6B. The data in Table 1 show that the spots from each region corresponded to CK, muscle isoform (spots 100−102), and GAPDH (spots 131−133), which are consistent with their theoretical pI and molecular weight.

To evaluate whether the changes observed in BisANS incorporation of CK and GAPDH translated into changes in function, the activities of these two enzymes were measured. As shown in Figure 7, the activities of both CK and GAPDH enzymes were reduced in response to oxidative stress. However, GAPDH was more sensitive than CK; e.g., the activity of GAPDH was abolished at iron/ascorbate concentrations above 1 μM iron/0.25 mM ascorbate (inset of Figure 7A), while the activity of CK remained unchanged until higher level of oxidative stress (5 μM iron/1.25 mM ascorbate).

Detection of Conformationally Altered Proteins in Denervated Skeletal Muscle using BisANS. We next determined if BisANS photoincorporation could detect changes in surface hydrophobicity of proteins *in vivo* after an oxidative stress. In these experiments, we used sciatic nerve denervation (as described in the Experimental Procedures) to generate oxidative stress in the skeletal muscle of mice. To confirm whether sciatic nerve denervation induces oxidative stress to skeletal muscle, we measured the release of hydrogen peroxide from isolated mitochondria fluoro-

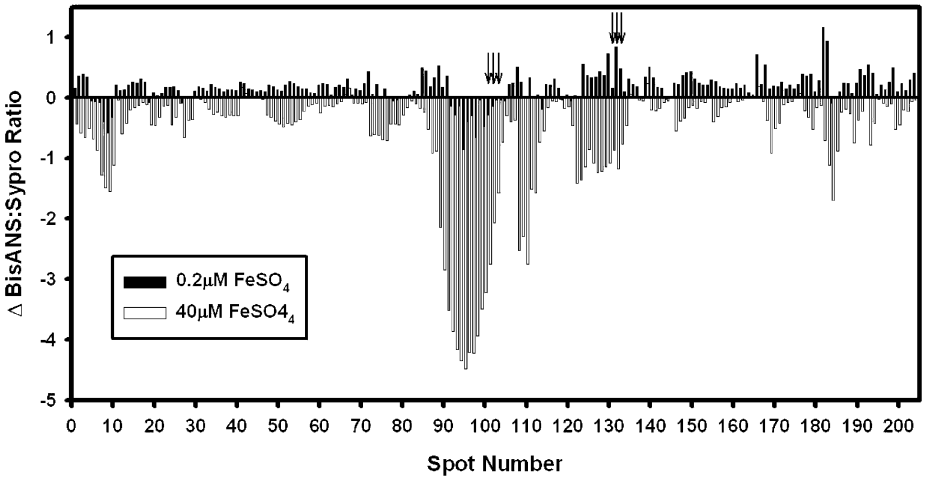

FIGURE 5: Quantification of changes in surface hydrophobicity in cytosolic proteins from skeletal muscle after oxidative stress. The data in Figure 4 were used to calculate changes in BisANS/Sypro Ruby fluorescence after low (black bars) or high (white bars) oxidative stress. The spots picked for MALDI−TOF/MS are indicated by arrows. Horizontal bars A and B indicate spots included in the two pI variants indicated in Figure 4.

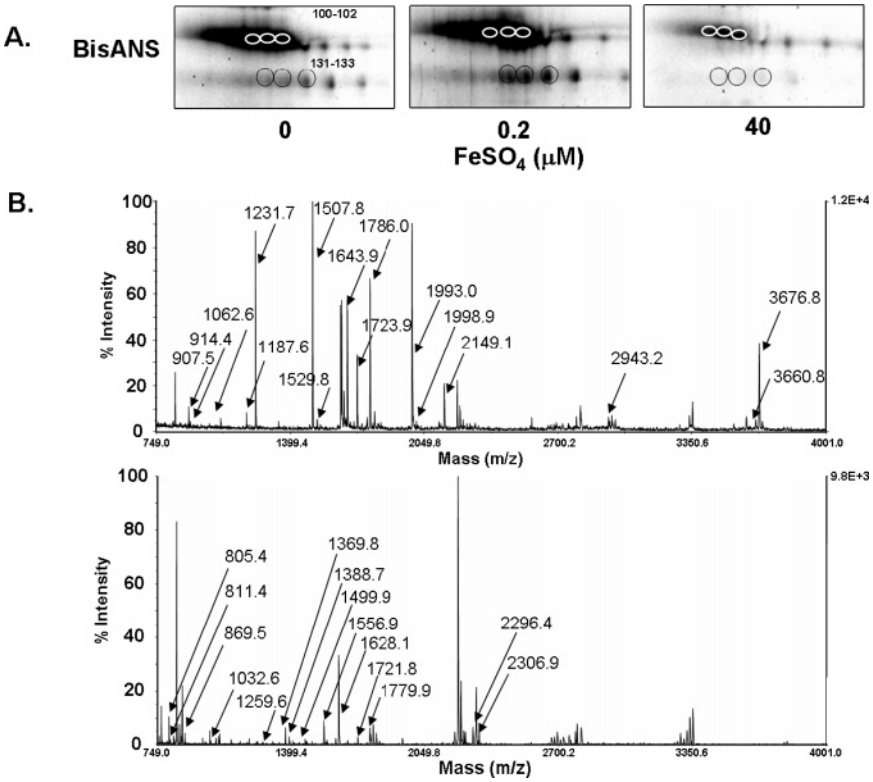

FIGURE 6: Identification of two skeletal muscle proteins showing changes in surface hydrophobicity after oxidative stress. (A) Enlargement of the region of the gels from Figure 4 showing the six spots (pI variant A, spots 100−102; and pI variant B, spots 131−133) that were taken for identification by MALDI−TOF/MS. (B) Representative spectra from pI variant A (top) and pI variant B (bottom) are shown. The arrows indicate the monoisotopic peaks of the matched peptides based on the mascot search.

Table 1: MALDI−TOF/MS Identification Summary

spot number	ID	$M_{r,calcd}$	pI_{calcd}	peptides searched	peptides matched	percent coverage (%)	expect	Mowse score
100	CK, muscle	43 018	6.58	20	13	33	2.6e−11	155
101	CK, muscle	43 018	6.58	27	10	29	2.2e−05	96
102	CK, muscle	43 018	6.58	35	16	49	6.6e−12	161
131	GAPDH	35 751	7.59	36	14	49	4.2e−09	133
132	GAPDH	35 751	7.59	51	16	51	2.1e−06	106
133	GAPDH	35 751	7.59	44	13	43	1.3e−06	108

metrically and found a marked increase in the release of hydrogen peroxide (17-fold) from the denervated muscle compared to control muscle tissue (data not shown). To determine whether proteins from denervated skeletal muscle show changes in surface hydrophobicity, we labeled cytosolic proteins from skeletal muscle of control and denervated mice

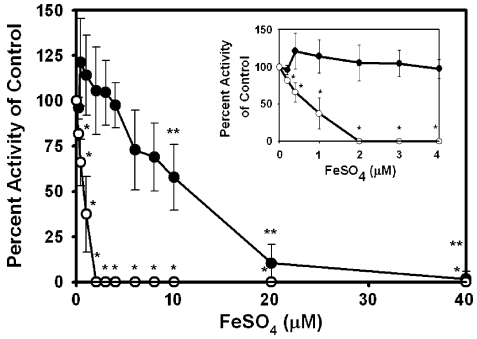

FIGURE 7: Effect of oxidative stress on the activities of CK and GAPDH. Cytosolic extracts from mouse skeletal muscle were exposed to various concentrations of iron (0, 0.2, 0.4, 1.0, 2.0, 3.0, 4.0, 6.0, 8.0, 10, 20, and 40 μM) and ascorbate (0, 0.05, 0.1, 0.25, 0.5, 0.75, 1, 1.5, 2, 2.5, 5, and 10 mM) for 1 h at 37 °C, and the activities of CK (●) and GAPDH (○) were measured as described in the Experimental Procedures. The data are expressed as the percent activity of the control (no oxidation) and represent the mean ± standard deviation obtained from three animals. (*) $p \leq 0.05$ versus the control.

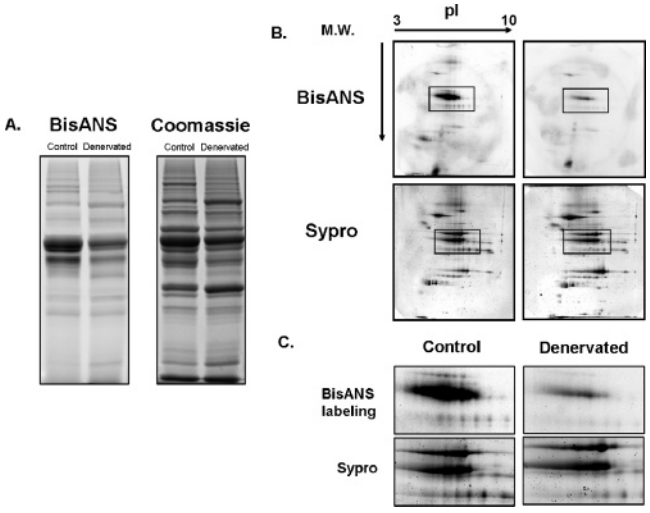

FIGURE 8: Screen of the skeletal muscle cytosol for changes in surface hydrophobicity after denervation. Cytosolic extracts from gastrocnemius muscles from control and denervated mice (1 mg/mL) were photolabeled with BisANS (100 μM), and the proteins were separated by 1D or 2D gel electrophoresis as described in the Experimental Procedures. (A) Image of the 1D gel showing the fluorescence from BisANS and Coomassie Blue staining. (B) Image of 2D gels showing the fluorescence from BisANS and Sypro Ruby. (C) Enlarged regions of the 2D gels shown boxed in B. Gels are representative of cytosolic extract pooled from two mice per group.

with BisANS, and the separation of proteins by 1D and 2D electrophoresis is shown in Figure 8. The 1D gels (Figure 8A) show a marked loss of incorporation of BisANS to two major protein bands in the region of CK and GAPDH. Upon 2D gel electrophoresis (Figure 8B), we also observed a major decrease in BisANS binding in the denervated skeletal muscle to the two pI variants previously identified as CK and GAPDH in the *in vitro* oxidative stress experiments (boxed). A slight decrease in Sypro Ruby staining can be observed in these two regions (Figure 8C); however, the ratio of BisANS/Sypro Ruby fluorescence decreased by 22 and 14% for CK and GAPDH compared to the control, respectively (data not shown). In addition, we measured the activities of CK and GAPDH in the control and denervated skeletal muscle from mice and observed that the activities of these two proteins decrease by more than 40% after denervation (data not shown).

DISCUSSION

Proteomics is becoming a powerful tool to screen the proteome of cells and tissues for changes in the expression of proteins. In addition to levels of expression, methods have also been developed to screen the proteome for post-translational modifications to proteins, e.g., phosphorylation (*30*), glycosylation (*31*), and oxidative modification (*32*, *33*). Post-translational modifications are important because they have been shown to alter the function/activity of proteins (*34, 35*) and often lead to an alteration of the protein structure (*5*). Because changes in the conformation of proteins can have a profound effect on the protein function, we were interested in developing an assay that would allow us to screen the proteome of a cell or tissue for changes in the conformation of specific proteins. We focused on surface hydrophobicity as a measure of protein conformation for two reasons. First, changes in surface hydrophobicity are often associated with deficits in protein function or aggregation, and second, the binding of the ANS compounds to proteins is a well-established assay for measuring the changes in surface hydrophobicity of purified proteins *in vitro* (*36*).

In this study, we took advantage of the ability of BisANS to covalently bind to the protein that it has interacted with after UV irradiation (*19*) and determined the relative amount of BisANS bound to specific proteins after gel electrophoresis. Using the mitochondrial matrix protein rhodanese as a model, we demonstrated that our assay was able to detect changes in surface hydrophobicity after treatment with urea. It is known that rhodanese adopts a molten globule form without aggregating after treatment with denaturants such as urea (*37*), which is associated with increased affinity to hydrophobic probes because of the exposure of more hydrophobic sites on its surface (*38*). As predicted, we observed an increase in BisANS incorporation in rhodanese following treatment with urea concentrations up to 2 M, likely because of the transition to the molten globule form. With concentrations of urea above 2 M, a loss of BisANS incorporation into rhodanese was observed because of the unfolding of ordered hydrophobic domains and destruction of BisANS binding sites (*39*, *40*).

Because changes in hydrophobic surfaces on proteins could be a sensitive marker for monitoring the changes in the protein structure (*17*, *41*), we determined if our assay could detect changes in the protein conformation caused by oxidative damage. For example, surface hydrophobicity is known to increase in rhodanese after chemical modification or oxidation of cysteine residues critical for maintaining rhodanese in a properly folded state (*39*, *40*). We showed that our assay was able to detect changes in the surface hydrophobicity of rhodanese after oxidative stress. A small increase in BisANS incorporation was observed at low levels of oxidative stress; however, at high levels of oxidative stress, a dramatic decrease in BisANS incorporation was observed that correlated with aggregation and partial unfolding as measured by light scattering and intrinsic tryptophan fluorescence, respectively. These data are consistent with a previous study by Horowitz and Criscimagna (*18*), showing the induction of aggregation of rhodanese from oxidation-

induced partial exposure of the surface hydrophobic domain. Therefore, our studies with a model protein, rhodanese, showed that our assay using photoincorporation of BisANS can detect changes in surface hydrophobicity that occur *in vitro*.

We tested the ability of our system to screen a mixture of proteins for changes in surface hydrophobicity by exposing the cytosolic proteins from skeletal muscle to various levels of oxidative stress. The changes in levels of incorporation of BisANS to skeletal muscle proteins with increasing oxidative stress was similar to that observed for rhodanese; e.g., at low levels of stress, a small increase in BisANS incorporation was observed, but at high levels of stress, a dramatic decrease in BisANS incorporation occurred. Using 2D gel electrophoresis, we determined the effect of oxidative stress on the incorporation of BisANS into over 200 cytosolic proteins in the skeletal muscle extracts. The effect of oxidative stress on BisANS incorporation and, therefore, surface hydrophobicity varied greatly from protein to protein, demonstrating the power of our assay to screen the proteome for changes in conformation. Some proteins showed very little change in BisANS incorporation in response to oxidative stress, while others proteins showed a dramatic alteration in BisANS incorporation. We identified two major skeletal muscle proteins that showed a large decrease in BisANS incorporation after high oxidative stress. These proteins are CK and GAPDH, which play an important role in energy homeostasis and metabolism in cells, respectively. CK maintains a "high-energy phosphate buffer" by catalyzing the reversible phosphorylation of creatine to phosphocreatine using adenosine triphosphate, while GAPDH is important in glycolysis and converts glyceraldehyde-3-phosphate to 1,3-bisphosphoglycerate. Thus, our data indicate that CK and GAPDH show reduced surface hydrophobicity in response to oxidative stress. To determine the functional significance of the changes in surface hydrophobicity, we measured the enzymatic activity of CK and GAPDH in the skeletal muscle extracts after exposure to oxidative stress. We observed that the activities of CK and GAPDH enzyme activity were lost after exposure to oxidative stress, which has been described previously (*42*, *43*).

Our long-range goal is to use the photoincorporation of BisANS to screen the proteome of cells/tissues for changes in surface hydrophobicity *in vivo* during normal and pathological processes. Therefore, we used our assay to screen cytosolic proteins of skeletal muscle from mice before and after denervation, a procedure that induces oxidative stress in skeletal muscle *in vivo*. We observed that BisANS incorporation to CK and GAPDH was dramatically reduced in skeletal muscle from denervated mice and that this reduced BisANS incorporation correlated with decreased enzymatic activity. Thus, oxidative stress *in vitro* and *in vivo* resulted in a decrease in surface hydrophobicity in CK and GAPDH, and this decrease in surface hydrophobicity has functional consequences. It is known that GAPDH utilizes a highly reactive cysteine in its active site and that oxidation of this cysteine *in vitro* by hydrogen peroxide can lead to alterations in quaternary structure (*43*, *44*). However, it is still unknown whether oxidation of cysteine 149 alone is sufficient to induce conformational changes that can be reported by BisANS. CK contains thiols in the active site of the enzyme as well (*45*), and conformational changes because of cysteine oxidation have been reported (*46*). However, differences in structural stability may explain the differential sensitivity observed with respect to enzyme activity and changes in conformation.

In summary, we have developed an assay that will allow investigators to screen the proteome of a cell/tissue for changes in surface hydrophobicity. Although assays have been developed to screen the proteome for changes in the levels of proteins or changes in post-translational modification, this is the first assay that will allow investigators to screen the proteome for changes in conformation. We believe that this assay will be a powerful tool that investigators can use in identifying potential protein targets that are involved in the molecular mechanism(s) underlying the progression of various pathological conditions because changes in exposure of hydrophobic domains on the surface of proteins often correlate with changes in protein function (*17*, *40*).

ACKNOWLEDGMENT

We thank the late Dr. Paul Horowitz, Department of Biochemistry, University of Texas Health Science Center at San Antonio, for his valuable comments and for providing us with pure rhodanese as a kind gift. It has been an honor to be his colleague. We also thank Fred Regnier and Richard Luduena for their comments and suggestions concerning the manuscript.

NOTE ADDED AFTER PRINT PUBLICATION

The name of Holly Van Remmen was published incorrectly in the version published on the Web February 7, 2006 (ASAP), and in the March 7, 2006, issue (Vol. 45, No. 9, pp 3077−3085). The correct electronic version of the paper was published April 6, 2006, and an Addition and Correction appears in the May 2, 2006, issue (Vol. 45, No. 17).

REFERENCES

1. Barroso, J. F., Carvalho, R. N., and Flatmark, T. (2005) Kinetic analysis and ligand-induced conformational changes in dimeric and tetrameric forms of human thymidine kinase 2, *Biochemistry 44*, 4886−4896.
2. LeMaster, D. M. (1990) Deuterium labelling in NMR structural analysis of larger proteins, *Q. Rev. Biophys. 23*, 133−174.
3. Acuna, A. U., Gonzalez-Rodriguez, J., Lillo, M. P., and Naqvi, K. R. (1987) Protein structure probed by polarization spectroscopy. I. Evidence for fibrinogen rigidity from stationary fluorescence, *Biophys. Chem. 26*, 55−61.
4. Panda, M., Ybarra, J., and Horowitz, P. M. (2002) Dissociation of the single-ring chaperonin GroEL by high hydrostatic pressure, *Biochemistry 41*, 12843−12849.
5. Meucci, E., Mordente, A., and Martorana, G. E. (1991) Metal-catalyzed oxidation of human serum albumin: Conformational and functional changes. Implications in protein aging, *J. Biol. Chem. 266*, 4692−4699.
6. Chapman, A. L., Winterbourn, C. C., Brennan, S. O., Jordan, T. W., and Kettle, A. J. (2003) Characterization of non-covalent oligomers of proteins treated with hypochlorous acid, *Biochem. J. 375*, 33−40.
7. Mahn, A., Lienqueo, M. E., and Asenjo, J. A. (2004) Effect of surface hydrophobicity distribution on retention of ribonucleases in hydrophobic interaction chromatography, *J. Chromatogr. A 1043*, 47−55.
8. Yamaguchi, S., Mannen, T., and Nagamune, T. (2004) Evaluation of surface hydrophobicity of immobilized protein with a surface plasmon resonance sensor, *Biotechnol. Lett. 26*, 1081−1086.
9. Chaudhuri, A. R., Seetharamalu, P., Schwarz, P. M., Hausheer, F. H., and Luduena, R. F. (2000) The interaction of the B-ring of

colchicine with α-tubulin: A novel footprinting approach, *J. Mol. Biol. 303*, 679−692.
10. Weber, G. (1952) Polarization of the fluorescence of macromolecules. II. Fluorescent conjugates of ovalbumin and bovine serum albumin, *Biochem. J. 51*, 155−167.
11. Martins, S. M., Chapeaurouge, A., and Ferreira, S. T. (2003) Folding intermediates of the prion protein stabilized by hydrostatic pressure and low temperature, *J. Biol. Chem. 278*, 50449−50455.
12. Erijman, L., Lorimer, G. H., and Weber, G. (1993) Reversible dissociation and conformational stability of dimeric ribulose bisphosphate carboxylase, *Biochemistry 32*, 5187−5195.
13. Lim, S. T., and Botts, J. (1967) Temperature and aging effects on the fluorescence intensity of myosin−ANS complex, *Arch. Biochem. Biophys. 122*, 153−156.
14. Poklar, N., Lah, J., Salobir, M., Macek, P., and Vesnaver, G. (1997) pH and temperature-induced molten globule-like denatured states of equinatoxin II: A study by UV-melting, DSC, far- and near-UV CD spectroscopy, and ANS fluorescence, *Biochemistry 36*, 14345−14352.
15. Almstedt, K., Lundqvist, M., Carlsson, J., Karlsson, M., Persson, B., Jonsson, B. H., Carlsson, U., and Hammarstrom, P. (2004) Unfolding a folding disease: Folding, misfolding, and aggregation of the marble brain syndrome-associated mutant H107Y of human carbonic anhydrase II, *J. Mol. Biol. 342*, 619−633.
16. Slavik, J. (1982) Anilinonaphthalene sulfonate as a probe of membrane composition and function, *Biochim. Biophys. Acta 694*, 1−25.
17. Horowitz, P. M., and Bowman, S. (1987) Conformational changes accompany the oxidative inactivation of rhodanese by a variety of reagents, *J. Biol. Chem. 262*, 8728−8733.
18. Horowitz, P., and Criscimagna, N. L. (1986) Low concentrations of guanidinium chloride expose apolar surfaces and cause differential perturbation in catalytic intermediates of rhodanese, *J. Biol. Chem. 261*, 15652−15658.
19. Seale, J. W., Brazil, B. T., and Horowitz, P. M. (1998) Photoincorporation of fluorescent probe into GroEL: Defining site of interaction, *Methods Enzymol. 290*, 318−323.
20. Sharma, K. K., Kumar, G. S., Murphy, A. S., and Kester, K. (1998) Identification of 1,1′-bi(4-anilino)naphthalene-5,5′-disulfonic acid binding sequences in α-crystallin, *J. Biol. Chem. 273*, 15474−15478.
21. Chao, C. C., Ma, Y. S., and Stadtman, E. R. (1997) Modification of protein surface hydrophobicity and methionine oxidation by oxidative systems, *Proc. Natl. Acad. Sci. U.S.A. 94*, 2969−2974.
22. Bradford, M. M. (1976) A rapid and sensitive method for the quantitation of microgram quantities of protein utilizing the principle of protein-dye binding, *Anal. Biochem. 72*, 248−254.
23. Laemmli, U. K. (1970) Cleavage of structural proteins during the assembly of the head of bacteriophage T4, *Nature 227*, 680−685.
24. Tanzer, M. L., and Gilvarg, C. (1959) Creatine and creatine kinase measurement, *J. Biol. Chem. 234*, 3201−3204.
25. Rafter, G. W., Chaykin, S., and Krebs, E. G. (1954) The action of glyceraldehyde-3-phosphate dehydrogenase on reduced diphosphopyridine nucleotide, *J. Biol. Chem. 208*, 799−811.
26. Harting, J., and Velick, S. F. (1954) Transfer reactions of acetyl phosphate catalyzed by glyceraldehyde-3-phosphate dehydrogenase, *J. Biol. Chem. 207*, 867−878.
27. Chappell, J. B., and Perry, S. V. (1954) Biochemical and osmotic properties of skeletal muscle mitochondria, *Nature 173*, 1094−1095.
28. Muller, F. L., Liu, Y., and VanRemmen, H. (2004) Complex III releases superoxide to both sides of the inner mitochondrial membrane, *J. Biol. Chem. 279*, 49064−49073.
29. Stadtman, E. R. (1992) Protein oxidation and aging, *Science 257*, 1220−1224.
30. Martin, K., Steinberg, T. H., Goodman, T., Schulenberg, B., Kilgore, J. A., Gee, K. R., Beechem, J. M., and Patton, W. F. (2003) Strategies and solid-phase formats for the analysis of protein and peptide phosphorylation employing a novel fluorescent phosphorylation sensor dye, *Comb. Chem. High Throughput Screening 6*, 331−339.
31. Steinberg, T. H., Pretty On Top, K., Berggren, K. N., Kemper, C., Jones, L., Diwu, Z., Haugland, R. P., and Patton, W. F. (2001) Rapid and simple single nanogram detection of glycoproteins in polyacrylamide gels and on electroblots, *Proteomics 1*, 841−855.
32. Aulak, K. S., Miyagi, M., Yan, L., West, K. A., Massillon, D., Crabb, J. W., and Stuehr, D. J. (2001) Proteomic method identifies proteins nitrated *in vivo* during inflammatory challenge, *Proc. Natl. Acad. Sci. U.S.A. 98*, 12056−12061.
33. Castegna, A., Aksenov, M., Aksenova, M., Thongboonkerd, V., Klein, J. B., Pierce, W. M., Booze, R., Markesbery, W. R., and Butterfield, D. A. (2002) Proteomic identification of oxidatively modified proteins in Alzheimer's disease brain. Part I: Creatine kinase BB, glutamine synthase, and ubiquitin carboxy-terminal hydrolase L-1, *Free Radical Biol. Med. 33*, 562−571.
34. Cabiscol, E., and Levine, R. L. (1995) Carbonic anhydrase III. Oxidative modification *in vivo* and loss of phosphatase activity during aging, *J. Biol. Chem. 270*, 14742−14747.
35. Oliver, C. N. (1987) Inactivation of enzymes and oxidative modification of proteins by stimulated neutrophils, *Arch. Biochem. Biophys. 253*, 62−72.
36. Grune, T., Reinheckel, T., and Davies, K. J. (1997) Degradation of oxidized proteins in mammalian cells, *FASEB J. 11*, 526−534.
37. Horowitz, P. M., and Butler, M. (1993) Interactive intermediates are formed during the urea unfolding of rhodanese, *J. Biol. Chem. 268*, 2500−2504.
38. Tandon, S., and Horowitz, P. M. (1990) The detection of kinetic intermediate(s) during refolding of rhodanese, *J. Biol. Chem. 265*, 5967−5970.
39. Panda, M., and Horowitz, P. M. (2000) Active-site sulfhydryl chemistry plays a major role in the misfolding of urea-denatured rhodanese, *J. Protein Chem. 19*, 399−409.
40. Bhattacharyya, A. M., and Horowitz, P. (2000) Alteration around the active site of rhodanese during urea-induced denaturation and its implications for folding, *J. Biol. Chem. 275*, 14860−14864.
41. Luduena, R. F., Roach, M. C., and Horowitz, P. (1986) The effects of the anilinonaphthalenesulfonates on the alkylation of tubulin: Correlation between the appearance of sulfhydryl groups and apolar binding sites, *Biochim. Biophys. Acta 873*, 143−146.
42. Suzuki, Y. J., Edmondson, J. D., and Ford, G. D. (1992) Inactivation of rabbit muscle creatine kinase by hydrogen peroxide, *Free Radical Res. Commun. 16*, 131−136.
43. Schmalhausen, E. V., Pleten, A. P., and Muronetz, V. I. (2003) Ascorbate-induced oxidation of glyceraldehyde-3-phosphate dehydrogenase, *Biochem. Biophys. Res. Commun. 308*, 492−496.
44. Arutyunova, E. I., Danshina, P. V., Domnina, L. V., Pleten, A. P., and Muronetz, V. I. (2003) Oxidation of glyceraldehyde-3-phosphate dehydrogenase enhances its binding to nucleic acids, *Biochem. Biophys. Res. Commun. 307*, 547−552.
45. Reddy, S., Jones, A. D., Cross, C. E., Wong, P. S., and van der Vliet, A. (2000) Inactivation of creatine kinase by S-glutathionylation of the active-site cysteine residue, *Biochem. J. 347* (part 3), 821−827.
46. Miura, T., Muraoka, S., and Fujimoto, Y. (2003) Inactivation of creatine kinase induced by quercetin with horseradish peroxidase and hydrogen peroxide. Pro-oxidative and anti-oxidative actions of quercetin, *Food Chem. Toxicol. 41*, 759−765.

BI052031I